Optical study of $Pr_{1-x}Ca_xMnO_3$ ($x=0.4$) in a magnetic field: Variation of electronic structure with charge ordering and disordering phase transitions

Y. Okimoto
Department of Applied Physics, University of Tokyo, Tokyo 113-8156, Japan
and Joint Research Center for Atom Technology (JRCAT), Tsukuba 305-0046, Japan

Y. Tomioka
Joint Research Center for Atom Technology (JRCAT), Tsukuba 305-0046, Japan

Y. Onose and Y. Otsuka
Department of Applied Physics, University of Tokyo, Tokyo 113-8156, Japan

Y. Tokura
Department of Applied Physics, University of Tokyo, Tokyo 113-8156, Japan
and Joint Research Center for Atom Technology (JRCAT), Tsukuba 305-0046, Japan
(Received 1 July 1998)

The temperature (10–290 K) and magnetic-field (0–7 T) dependencies of optical spectra and their anisotropy have been investigated for a single crystal of $Pr_{1-x}Ca_xMnO_3$ ($x=0.4$), which undergoes a charge and orbital ordering transition at $T_{co}=235$ K. A clear anisotropic feature has been observed between the *b*- and *c*-axis polarized optical conductivity spectra [$\sigma(\omega)$] at 10 K, reflecting a pattern of spatial charge and orbital ordering. The gap value of the charge-ordered (CO) state is estimated to be ≈ 0.18 eV in the ground state. $\sigma(\omega)$ is drastically transformed from an anisotropic gaplike shape into an isotropic metallic band with a conspicuous spectral weight transfer over a wide photon energy region (0.05–3 eV) by application of a magnetic field of 7 T. As the magnetic field is decreased from 7 T, such metallic $\sigma(\omega)$ suddenly becomes gaplike again around 4.5 T, yet the anisotropy between both polarizations is decreased perhaps owing to orbital disordering. The temperature dependence of the *b*-axis polarized $\sigma(\omega)$ was investigated in a constant magnetic field of 7 T. As the temperature decreases, the onset energy of $\sigma(\omega)$ shows a blueshift from T_{co} down to the antiferromagnetic spin ordering temperature T_N, but shows a redshift once the spin ordering takes place below T_N. This result indicates that the charge gap value as the order parameter of the CO state couples with the spin ordering. [S0163-1829(99)01312-0]

I. INTRODUCTION

Spin-charge-orbital-coupled phenomena in hole-doped manganese oxides with a perovskite structure have been attracting great interest in recent extensive studies. One of the most intriguing features observed in these manganites is a large magnetoresistance (MR) effect. The $La_{1-x}Sr_xMnO_3$ system is, for example, the most canonical double-exchange manganite with a wide one-electron bandwidth (W), and shows a ferromagnetic metallic (FM) state[1] ($x>0.15$) as well as a large MR effect around the Curie temperature (T_c).[2–9] An origin of the FM state and the relatively large MR effect around T_c has been explained in terms of a double-exchange mechanism.[10–14] It has been pointed out that a Jahn-Teller distortion is also an important key to the colossal MR effects of the manganites.[15,16] Such a FM state is, however, absent in the more distorted perovskite $Pr_{1-x}Ca_xMnO_3$ ($0.3\leqslant x\leqslant 0.5$) system that has a smaller W and which undergoes a charge ordering phase transition.[17,18] In the charge-ordered (CO) state, Mn^{3+} and Mn^{4+} are alternately arranged with spin and orbital ordering.[17] Recently, Tomioka *et al.* revealed that the CO state can be melted into a FM one with a drastic decrease of resistivity by applying a magnetic field of a T,[19] and that such a magnetic-field-induced insulator-metal (I-M) transition is of the first order with a large field hysteresis. It has been demonstrated since then, especially for the $Pr_{1-x}Ca_xMnO_3$ system, that such charge ordering and disordering transitions can be caused by external stimuli other than a magnetic field, e.g., x-ray irradiation,[20] illumination by a pulsed laser,[21,22] and current injection.[23] Here we adopt a crystal of $Pr_{1-x}Ca_xMnO_3$ ($x=0.4$) as a prototypical charge ordering system, and investigate the variation of the electronic structure from the CO insulating state to a FM one in terms of optical spectra while varying temperature and the external magnetic field.

To overview the transport and magnetic properties of this particular crystal, in Fig. 1(a) we introduce the phase diagram for $Pr_{1-x}Ca_xMnO_3$ ($x=0.4$) in the temperature and magnetic plane.[18] In a zero magnetic field, the $x=0.4$ compound undergoes a charge ordering phase transition at $T_{co}\approx 235$ K. In the CO state, the nominal Mn^{3+} and Mn^{4+} species are regularly arranged in the ab plane with a concomitant ordering of $d_{3x^2-r^2}$ and $d_{3y^2-r^2}$ orbitals, as shown in Fig. 1(b). This was directly confirmed by x-ray scattering measurements using the anisotropy of the tensor of susceptibility reflection.[24] From neutron-diffraction results by Jirak *et al.*[17] it was concluded that the extra electrons resulting from a deviation in doping level x from $x=\frac{1}{2}$ (0.1 per Mn site in the present $x=0.4$ case) are likely to occupy a $d_{3z^2-r^2}$ orbital in the Mn^{4+} site. As temperature is decreased, anti-

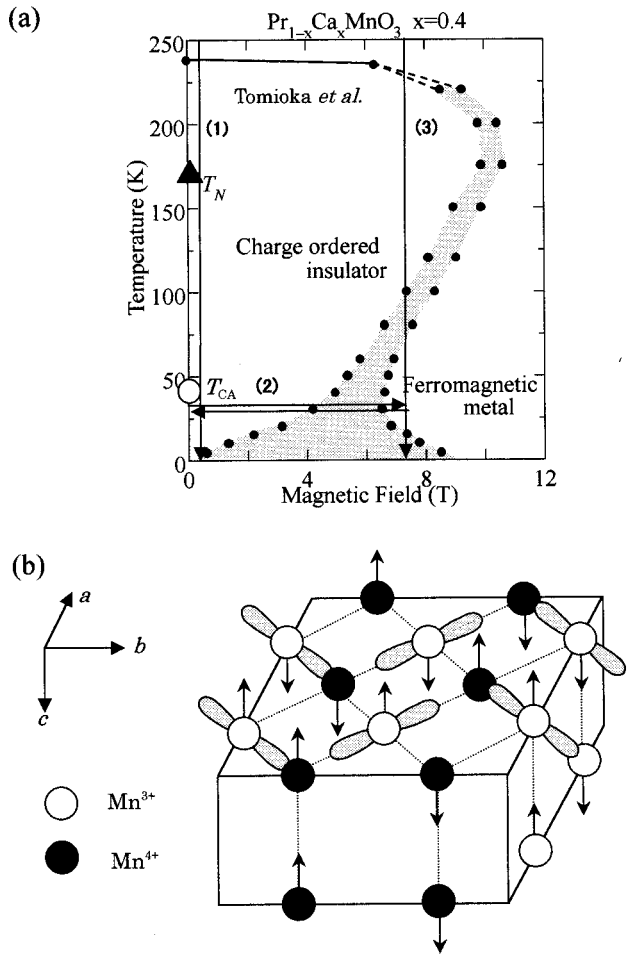

FIG. 1. (a) The temperature and magnetic phase diagram of $Pr_{1-x}Ca_xMnO_3$ ($x=0.4$) derived from Ref. 18. The hatched area shows a field-hysteresis region. A closed triangle denotes the Néel temperature T_N, and an open circle the canted antiferromagnetic transition temperature T_{CA}. The three routes (1)–(3) for the temperature or magnetic-field scans adopted in the present study are displayed. (b) Modified *CE*-type spin and charge ordering structure. The lobes show the $d_{3x^2-r^2}$ or $d_{3y^2-r^2}$ orbital (see text).

ferromagnetic spin ordering of the *CE* type[17,25] subsequently takes place at $T_N \approx 170$ K, as indicated by the closed triangle in Fig. 1(a). (To be precise, the direction of the spin is declined out of the *c* axis by 20°–30° in the $x=0.4$ compound.[17]) It is worth noting that the *CE*-type spin structure for the $x=0.4$ compound contains ferromagnetically spin-aligned chains along the *c* axis [see Fig. 1(b)]. This feature is in contrast to the *antiferromagnetic* chain along the *c* axis seen in the commensurate CO compound $Pr_{1/2}Ca_{1/2}MnO_3$ ($x=1/2$).[17] Such a ''ferromagnetic'' spin ordering along the *c* axis probably results from the extra electrons whose hopping aligns t_{2g} spins in the Mn^{4+} site via the double-exchange process. With further decrease in temperature below T_N, the canted antiferromagnetic (CA) ordering is achieved at $T_{CA} \approx 40$ K [the open circle in Fig. 1(b)]. In the external magnetic field, the charge-ordered (CO) state is transformed into a ferromagnetic metallic state by way of a hesteretic region shown by the hatched region in Fig. 1(a). Such a large field hysteresis indicates the distinct first-order nature of the field-induced *I-M* transition in the $Pr_{1-x}Ca_xMnO_3$ system.

Some results of our research (the magnetic-field dependence of reflectivity spectra at 30 K) have been published in a form of a short communication.[26] In the present paper, we present full results of systematic optical measurements in $Pr_{1-x}Ca_xMnO_3$ ($x=0.4$), and discuss the variation of electronic structures with charge ordering and disordering transitions together with the results of magnetotransport measurements. In Sec. II, we describe the experimental procedure for optical measurements in magnetic fields and that for sample preparation and characterization. In Sec. III A, we discuss the anisotropic electronic structure of the CO state at 10 K in 0 T, which can be viewed as representing a ground state, and its temperature dependence along route (1) shown in the upper panel of Fig. 1. In Sec. III B, we show the magnetic-field dependence of optical spectra at 30 K in field-increased and -decreased runs [route (2)]. In Sec. III C, we describe and discuss the temperature dependence of optical spectra in 7 T [route (3)]. All three routes (1)–(3) in the phase diagram can cause the charge ordering and disordering transitions. Finally, in Sec. IV, we summarize the paper.

II. EXPERIMENT

The specimen of $Pr_{1-x}Ca_xMnO_3$ ($x=0.4$) used in this study was a single crystal melt grown by a floating-zone method, the details of which have been reported elsewhere.[19] Application of an electron probe microanalyzer and chemical titration have confirmed that the obtained crystal has precisely prescribed stoichiometry. The sample ($\approx 4\times 5\times 0.5$ mm^3) with a [1 0 0] surface (*Pbnm* orthorhombic structure) was prepared by Laue and four-circle x-ray diffraction. Near-normal-incidence reflectivity [$R(\omega)$] was measured on this [1 0 0] surface. We made use of a Fourier-transform-type spectrometer with a MCT (HgCdTe) detector for the region from 0.05 to 0.8 eV and grating monochromators for the higher-energy region (0.6–36 eV). For the spectroscopy above 5 eV, we utilized synchrotron radiation at INS-SOR, Institute for Solid State Physics, University of Tokyo. In zero magnetic field, we measured $R(\omega)$ between 0.01 and 3 eV while varying temperature ($10\ \mathrm{K} < T < 290\ \mathrm{K}$) using a He flow-type cryostat.

High-magnetic-field measurements ($0\ \mathrm{T} < H < 7\ \mathrm{T}$) of $R(\omega)$ between 0.05 and 3 eV were performed with a split-type superconducting magnet equipped with ZnSe and KRS-5 windows for infrared spectroscopy and quartz ones for measurements in the visible photon energy region. We measured $R(\omega)$ in Voigt geometry ($\mathbf{k}\perp\mathbf{H}$) from 0.05 to 0.8 eV, and in Faraday geometry ($\mathbf{k}\parallel\mathbf{H}$) from 0.6 to 3 eV, and applied the magnetic field along the *b* axis of the *Pbnm* orthorhombic lattice [see Fig. 1(b)]. The optical conductivity spectra at various temperatures and magnetic fields were obtained by Kramers-Kronig (KK) analysis of respective $R(\omega)$ data. For the analysis, we connected the room-temperature datum above 3 eV, which is no longer sensitive, to variations of the respective data at various temperatures and magnetic fields, and assumed constant reflectivity below the lowest photon energy investigated and ω^{-4} extrapolation above 36 eV. In executing the KK analysis, we neglected the influence of a magneto-optical Kerr effect, namely, an off-diagonal

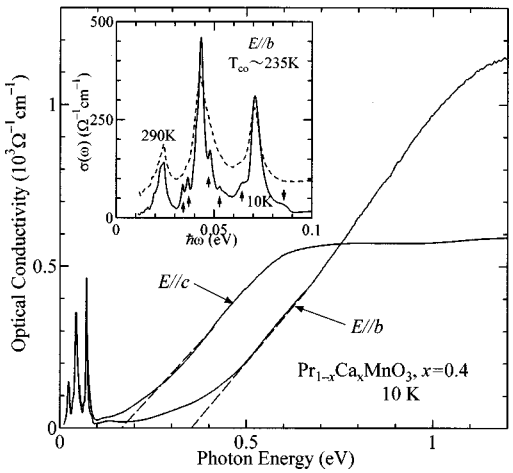

FIG. 2. The anisotropy ($\mathbf{E}\|b$ and $\mathbf{E}\|c$ polarization) of the optical conductivity in a single crystal of $Pr_{1-x}Ca_xMnO_3$ ($x=0.4$) at 10 K. Long dashed lines indicate the estimate of the gap transition energies (see text). The inset shows a magnification of the far-infrared photon energy region.

component of dielectric tensor $[\epsilon_{xy}(\omega)]$. This is because the magnitude of $\epsilon_{xy}(\omega)$ in the low-energy (<4 eV) region is much smaller than that of diagonal part,[27] and also because there is no orbital moment for the conduction e_g electrons and hence minimal spin-orbit coupling. Magnetization measurements were performed with a superconducting quantum interference device magnetometer, and resistivity in the magnetic field was measured by the conventional four-probe technique.

III. RESULTS AND DISCUSSION

A. Temperature dependence of optical spectra in 0 T

Figure 2 shows the optical conductivity spectrum $[\sigma(\omega)]$ in $Pr_{1-x}Ca_xMnO_3$ ($x=0.4$) for $\mathbf{E}\|b$ and $\mathbf{E}\|c$ at 10 K. (Spiky structures below 0.06 eV are due to optical-phonon modes.) In the CO state at 10 K (viewed as the ground state), there is a clear difference between the b- and c-axis polarized $\sigma(\omega)$, reflecting the anisotropy of the ordering pattern for charge, spin, and orbitals [see Fig. 1(b)]. The most notable feature is that each $\sigma(\omega)$ has a different onset energy (Δ). To be more quantitative, we have estimated each Δ (Δ_b and Δ_c) by linearly extrapolating the rising part of the b- and c-axis polarized $\sigma(\omega)$ to the abscissa, as shown by dashed lines in Fig. 2. It is reasonable to consider that Δ_b is dominated by the optical transition of the $d_{3x^2-r^2}$ (or $d_{3y^2-r^2}$) electron to the neighboring Mn^{4+} site along the direction of the orbital [see Fig. 1(b)]. The $d_{3x^2-r^2}(d_{3y^2-r^2})$ electron can hardly hop along the c axis due to a small transfer integral and a large on-site Coulomb energy. As mentioned above, the excess electrons which are introduced into the CE-type CO state by decreasing x from $\frac{1}{2}$ are likely to occupy the $d_{3z^2-r^2}$ orbital of the Mn^{4+} site[17] with a large transfer integral along the c axis, indicating that Δ_c originates from the intersite transition of such excess $d_{3z^2-r^2}$ electrons. The fact that $\Delta_c<\Delta_b$ implies that the effective Coulomb correlation is larger within the ab plane than along the c axis.Under these circumstances, the charge-gap energy ($2\Delta_{gap}$) should be assigned to Δ_c (≈ 0.18 eV) in the ground state.

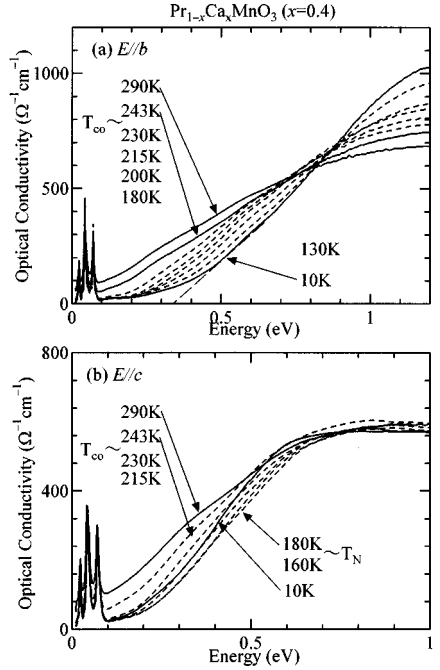

FIG. 3. The temperature variation of the optical conductivity spectra in a single crystal of $Pr_{1-x}Ca_xMnO_3$ ($x=0.4$) for (a) $\mathbf{E}\|b$ and (b) $\mathbf{E}\|c$ polarizations. A dashed line indicates the estimate of the gap transition energies (see text).

In the inset of Fig. 2 we also show the optical-phonon spectra at 10 K (290 K) with a solid (dashed) line. At 290 K, there are observed three dominant phonon modes at 0.023, 0.042, and 0.071 eV. By contrast, at least six additional phonon modes, as indicated with arrows, emerge at 10 K (i.e., in the CO ground state). One of the origins of the apparently new modes is considered to be $Pbnm$ orthorhombic distortion. With a decrease in temperature, thermally blurred phonon structures at room temperature might become sharpened and discernible due to a decrease in phonon damping as well as to a missing Drude component [see Fig. 3(a)]. However, the three evident phonon structures at 293 K indicate that the orthorhombic distortion of the crystal is relatively small considering that only three ($3F_{2u}$) modes are infrared active in a cubic perovskite in contrast to 25 optical-phonon modes ($7B_{1u}+9B_{2u}+9B_{3u}$) in the $Pbnm$ orthorhombic one according to a group analysis.[28] Furthermore, the highest-lying phonon mode around 0.086 eV, to the best of our knowledge, has never been observed in simply orthorhombically distorted manganites. These results suggest that orthorhombicity alone can hardly explain such a remarkable increase in the number of observable phonon modes. Another explanation is the charge ordering phase transition. The CE-type charge and orbital ordering, as shown in Fig. 1(b), forms a superlattice along the b axis, so that new Γ point modes appear on account of foldings of phonon-dispersion branches. Such multiplet phonon features due to the CE-type charge ordering are also observed in two-dimensional manganite, $La_{3/2}Sr_{1/2}MnO_4$.[29]

Next let us discuss the temperature dependence of $\sigma(\omega)$ from 10 K up to room temperature. Figures 3(a) and 3(b) show the temperature dependence of optical conductivity

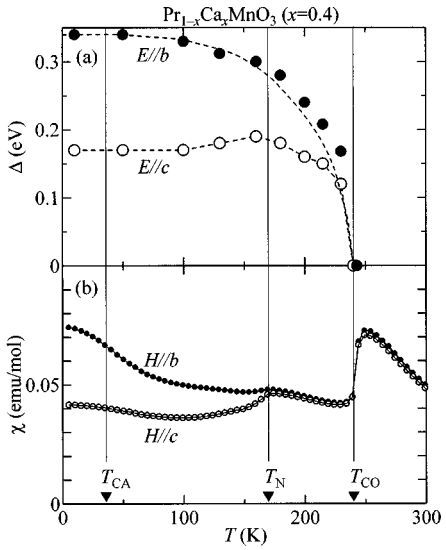

FIG. 4. (a) The temperature dependence of energies of a polarized gap transition, Δ_b (closed circle) and Δ_c (open circle), in a $Pr_{1-x}Ca_xMnO_3$ ($x=0.4$) crystal. (b) The temperature dependence of the magnetic susceptibility χ and its anisotropy.

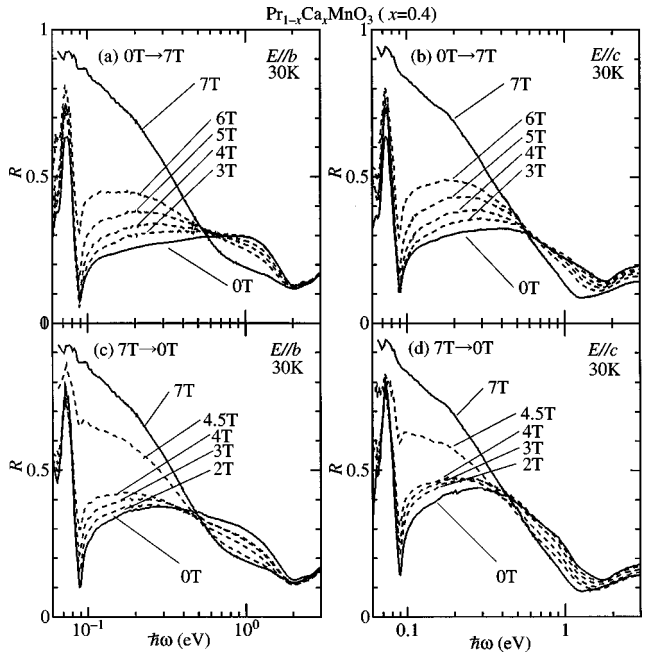

FIG. 5. The magnetic-field dependence of the reflectivity spectra in the field-increased run for (a) $\mathbf{E}\|b$ and (b) $\mathbf{E}\|c$ polarizations and in the field-decreased run for (c) $\mathbf{E}\|b$ and (d) $\mathbf{E}\|c$ for a $Pr_{1-x}Ca_xMnO_3$ ($x=0.4$) crystal at 30 K.

spectra (10–293 K) in $Pr_{1-x}Ca_xMnO_3$ ($x=0.4$) for $\mathbf{E}\|b$ and $\mathbf{E}\|c$, respectively. With an increase in temperature from 10 K to T_{co}, the onset energy of $\sigma(\omega)$ shifts to lower energy. Above T_{co} ($=235$ K), the spectral weight is largely increased in the lower-energy part, and the spectral shape becomes gapless implying a closing of the charge gap. Such a temperature dependence of $\sigma(\omega)$ resembles that of the $La_{5/3}Sr_{1/3}NiO_4$ CO system.[30] On the other hand, the onset of c-polarized $\sigma(\omega)$ moves to higher energy, similar to the b-polarized case with a decrease in temperature from T_{co} ($=235$ K) to T_N ($=170$ K), but shifts to a rather lower energy below T_N. [The c-polarized $\sigma(\omega)$ at 10 K is drawn, for clarification, with a bold line in Fig. 3(b).] This result indicates that magnetic ordering affects gap evolution in c-polarized optical spectra.

We estimated the Δ value by a linearly extrapolating procedure, as shown by dot-dashed lines in Figs. 2 and 3(a). Figure 4(a) shows Δ values thus obtained as a function of temperature. For comparison, the temperature dependence of magnetic susceptibility (χ) is shown in Fig. 4(b). Above T_{co}, the magnitude of χ is fairly large due to the double-exchange mechanism. Once charge ordering occurs ($T<T_{co}$), however, the χ value is abruptly suppressed because of quenching of double-exchange interaction in the CO state. Anisotropy of the magnetic susceptibility is clearly observed in the temperature region below T_N, while scarcely observed in the paramagnetic state ($T>T_N$). The χ measured in $\mathbf{H}\|c$ is lower with a cusp structure at T_N, but in $\mathbf{H}\|b$ it is almost constant below T_N, indicating that an easy axis of sublattice magnetization is approximately parallel to the c axis. (The increase in χ below $T\approx100$ K is due to the canted antiferromagnetic spin order.[25]) These results are consistent with those of neutron-scattering measurements.[17]

Keeping the above in mind, we discuss the T dependence of the anisotropic Δ value [Fig. 4(a)]. In the entire temperature region below T_{co}, the Δ_c values are always smaller than Δ_b. With decreasing temperature, Δ_b increases monotonically and is scarcely affected by the antiferromagnetic spin ordering in the ab plane. By contrast, Δ_c decreases significantly below T_N. This might be because the c-axis hopping of the excess $d_{3z^2-r^2}$ carriers is favored by the ferromagnetic spin ordering along the c axis below T_N [see Fig. 1(b)] as a consequence of one-dimensional (along the c axis) double-exchange interaction in the *electron-doped* CO state ($x<0.5$).

B. Magnetic-field dependence of optical spectra at 30 K

The next issue to be highlighted is the collapse and reconstruction of the gap structure in magnetic field-increased and -decreased runs for a $Pr_{1-x}Ca_xMnO_3$ ($x=0.4$) crystal at 30 K [see route (2) in Fig. 1(a)]. In Figs. 5(a) and 5(b) we show the magnetic-field dependence of $R(\omega)$ at 30 K in the field-increased process ($0\rightarrow7$ T) for $\mathbf{E}\|b$ and $\mathbf{E}\|c$, respectively. A spiky structure around 0.06 eV is due to the highest-lying oxygen phonon mode. In both the b- and c-polarized $R(\omega)$, a midinfrared part of $R(\omega)$ is gradually increased with a magnetic field up to 6 T, and the spectral shape is abruptly transformed into a metallic high-reflectivity band between 6 and 7 T. This value of the critical field is consistent with the phase diagram in Fig. 1(a).[18] Such a spectral change with an external magnetic field over a wide photon energy region up to ≈3 eV is very unconventional, taking the small energy of the magnetic field (1 T$\approx8.6\times10^{-4}$ eV) into account. The quantity of the spectral weight transfer is by far larger than that observed near the ferromagnetic transition temperature in $Nd_{0.7}Sr_{0.3}MnO_3$ thin film.[31]

In Figs. 5(c) and 5(d) we also show $R(\omega)$ in the field-decreased run ($7\rightarrow0$ T) for $\mathbf{E}\|b$ and $\mathbf{E}\|c$, respectively. The metallic reflectance band for both polarizations largely decreases between 5 and 4 T, and the spectral shape is gradu-

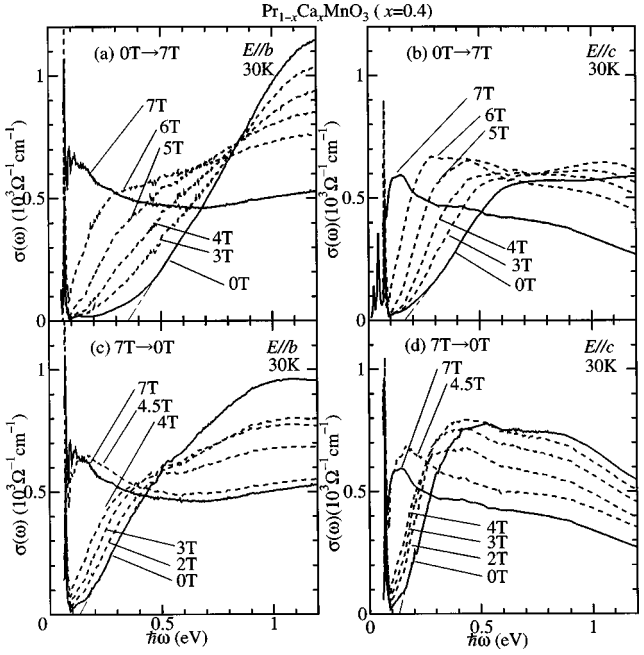

FIG. 6. The magnetic-field dependence of the optical conductivity spectra in the field-increased run for (a) $\mathbf{E}\|b$ and (b) $\mathbf{E}\|c$ polarizations, and in the field-decreased run for (c) $\mathbf{E}\|b$ and (d) $\mathbf{E}\|c$ for a $Pr_{1-x}Ca_xMnO_3$ ($x=0.4$) crystal at 30 K deduced by Kramers-Kronig analysis. Dot-dashed lines indicate the estimate of the gap transition energies (see text).

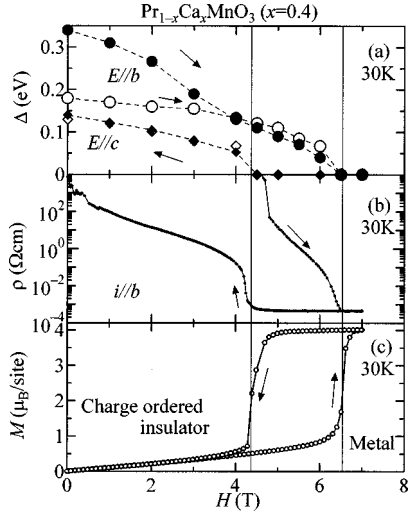

FIG. 7. (a) The magnetic-field dependence of Δ_b (closed symbols) and Δ_c (open symbols) in the field-increased run (circles) and field-decreased run (squares) for a $Pr_{1-x}Ca_xMnO_3$ ($x=0.4$) crystal at 30 K. (b) The magnetic-field dependence of the resistivity (ρ). (c) The magnetic-field dependence of the magnetization (M).

ally restored toward an initial spectral shape below 4 T. To see such a hysteretic spectral change with the magnetic field more quantitatively, we show in Fig. 6(a) [6(b)] the b- [c-] polarized $\sigma(\omega)$ deduced by KK analysis and their magnetic-field dependence at 30 K. With an increase in the magnetic field, the onset of $\sigma(\omega)$ gradually shifts to a lower energy, and at 7 T $\sigma(\omega)$ undergoes a large change into a metallic band, as expected from the variation of $R(\omega)$. All the optical conductivity spectra below 6.5 T are gapped, with little spectral weight below the respective onset energies (except for optical-phonon components), while the rapid and remarkable transfer of the spectral weight to a lower (but not as far as zero) energy with the magnetic field is observed even in the insulator region. This is reminiscent of the doped Mott insulator case including a high-T_c cuprate,[32,33] where the spectral weight is gradually accumulated below the photon energy of an isosbetic point (approximately corresponding to a gap value in the parent insulator) with hole doping. The spectrum above 7 T may have a Drude weight (coherent part), but it is still too small to estimate the exact weight from present data ($0.05\ \text{eV}<\hbar\omega<3\ \text{eV}$) due to the more dominant diffusive (incoherent) spectral shape. (The value of the dc conductivity [$\sigma(0)$] at 30 K and 7 T is $\approx 2\times 10^3\ \Omega^{-1}\,\text{cm}^{-1}$ [see Fig. 7(b)], which is merely about twice that of $\sigma(\omega)$ at 0.06 eV.) This incoherent spectral feature of the FM phase is consistent with that of the $La_{1-x}Sr_xMnO_3$ system near the metal-insulator phase boundary ($x=0.175$).[34] In the field-decreased run, such metallic spectra for both polarizations ($\mathbf{E}\|b$ and $\mathbf{E}\|c$) dramatically return to the gaplike one between 4 and 5 T, as shown in Figs. 6(c) and 6(d). With a further decrease in the magnetic field below 4 T, the onset energy Δ of $\sigma(\omega)$ shows a gradual and small increase. The final spectral shape of $\sigma(\omega)$ at 0 T never returns to the initial one with a large anisotropy (see Fig. 2).

Here we have again estimated the Δ value as a measure of the charge-transfer energy reflecting charge, spin, and orbital ordering by means of the same extrapolating procedure as mentioned above (see Figs. 2 and 3). In Fig. 7(a) we show a variation of Δ value with magnetic field at 30 K for both the field-increased and -decreased runs. For comparison, in Figs. 7(b) and 7(c) we show the magnetic-field dependence of resistivity (ρ) along the b axis and magnetization (M) at 30 K, respectively. In both the ρ and M measurements, the applied magnetic field was parallel to the b axis as in the optical measurements. As shown, $\rho(M)$ steeply drops (increases) around 6.5 T in the field-increased run. Above 6.5 T, M shows a nearly full moment ($\approx 4\mu_B$), and the ρ value is metallic ($\approx 5\times 10^{-4}\ \Omega\,\text{cm}$) and is no longer affected by further increase of the field, indicating the fully spin-polarized FM state. In the field-decreased run, $\rho(M)$ steeply increases (drops) below ≈ 4.2 T, where a high antiferromagnetic insulating state is realized. It is worth noting that ρ does not return to the starting value, which is too high to measure accurately, while M below 4.2 T in the field-decreased run reproduces the value observed in the field-increased run. As mentioned above, Δ_b is greater than Δ_c (30 K, 0 T) by 0.18 eV. This difference is gradually decreased with a magnetic field, and both the Δ_b and Δ_c values decrease almost continuously down to zero at 6.5 T in the field-increased run. These results clearly indicate that the order parameter of the CO state continuously decreases, and the anisotropy of Δ is suppressed with the magnetic field. In the field-decreased run from 7 T, the Δ value appears between 3 and 4 T, again in accordance with the critical field of ρ and M. However, Δ_b and Δ_c are rather comparable and obviously less than Δ_c in the field-increased run. One might consider that the small value of Δ and ρ in the zero-field state after the field-decreased run results from coexistence of FM domains in the insulating state due to the strong first-order nature of the present charge ordering and disordering

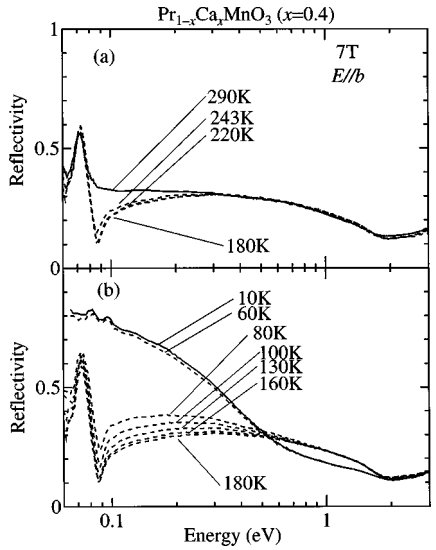

FIG. 8. The temperature variation of the b-polarized reflectivity spectra for a $Pr_{1-x}Ca_xMnO_3$ ($x=0.4$) crystal in a magnetic field of 7 T: (a) 180 K$<T<$290 K, and (b) 10 K$<T<$180 K.

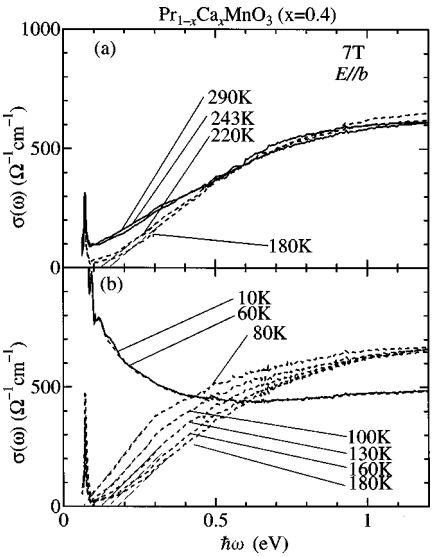

FIG. 9. The temperature variation of the optical conductivity spectra in $Pr_{1-x}Ca_xMnO_3$ ($x=0.4$) for $\mathbf{E}\|b$ polarization in a magnetic field of 7 T: (a) 180 K$<T<$290 K and (b) 10 K$<T<$180 K. Dot-dashed lines indicate the estimate of the gap transition energies (see text).

transitions. However, the striking decrease and reproducibility of the M-value in the field-decreased run below 4.2 T suggest that the FM component is, if anything, very minor in the final CO state. A possible origin of these irreversible behaviors of ρ and Δ may be ascribed to the fact that the $d_{3x^2-r^2}$ and $d_{3y^2-r^2}$ orbital ordering are not completely restored in the field-decreased run, so that the robustness of the CO state may be weakened by such an orbital disordering effect. To confirm the hypothesis, further studies such as by resonant x-ray scattering measurements in the magnetic field would be needed.

C. Temperature dependence of optical spectra in 7 T

In this section, we discuss the temperature dependence of optical spectra for $\mathbf{E}\|b$ in a magnetic field of 7 T in $Pr_{1-x}Ca_xMnO_3$ ($x=0.4$) [see route (3) in Fig. 1(a)]. Figure 8 shows the b-axis polarized $R(\omega)$ and its temperature dependence at 7 T. (The spiky structures around 0.08 eV are the highest-lying optical phonon mode, as mentioned above.) With a decrease in temperature from 290 to 180 K, the midinfrared (0.1–0.5 eV) part of $R(\omega)$ shows a gradual decrease, as shown in Fig. 8(a). By contrast, the midinfrared $R(\omega)$ gradually increases from 180 to 70 K, and finally changes into a metallic band below 60 K [Fig. 8(b)].

To argue such a nonmonotonous temperature dependence of the electronic structure, in Fig. 9 we show the temperature dependence of $\sigma(\omega)$ in a magnetic field of 7 T. The lower-energy part of $\sigma(\omega)$ is suppressed, and becomes more gaplike with a decrease in temperature from 290 to 180 K [Fig. 9(a)], while the onset energy of the absorption shows a gradual redshift with a further decrease in temperature down to 60 K [Fig. 9(b)]. Such a variation of the b-axis polarized $\sigma(\omega)$ is in striking contrast to that observed in the zero-field-cooled run [see Figs. 3 and 4(a)] in which the spectra $\sigma(\omega)$ remains gaplike down to 10 K. $\sigma(\omega)$ drastically turns into a metallic band below 60 K that is in accord with a critical temperature at 7 T for the transition from the CO state to the FM state.[18] The metallic spectral shape comparable with that seen in the field-increased run at 30 K [cf. Fig. 6(c)] is then scarcely changed down to 10 K.

We have again estimated the charge-transfer energy Δ_b using the same extrapolating procedure as shown by dashed lines in Fig. 9. In Fig. 10(a) we plot the temperature dependence of Δ_b in comparison with that of ρ and M in Figs. 10(b) and 10(c), respectively. The value of ρ in 7 T shows an abrupt increase, while M is suppressed around $\approx$230 K due to the charge ordering phase transition. With a further decrease in temperature, the ρ value increases up to 100 K, and finally shows a drastic decrease at $\approx$60 K. The value of M shows a small cusp structure around T_N (170 K), as shown by the arrow, and a sudden increase at a temperature of 60 K.

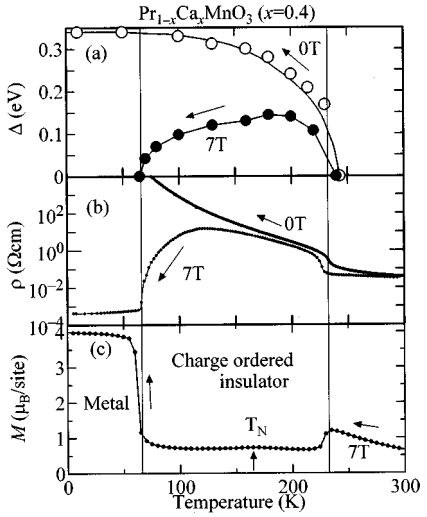

FIG. 10. (a) The temperature dependence of the energies of the polarized gap transition (Δ_b) for a $Pr_{1-x}Ca_xMnO_3$ ($x=0.4$) crystal in a magnetic field of 7 T. (b) The temperature dependence of the resistivity ρ at 0 T (open circles) and 7 T (closed ones). (c) The temperature dependence of the magnetization (M) at 7 T.

In the low-temperature state below 60 K, $\rho \approx 5 \times 10^{-4}$ Ω cm and $M \approx 4\mu_B$, indicating that the FM state is realized due to the reentrant melting of the CO state. Such temperature-induced charge ordering and disordering transitions are sensitively reflected in the temperature variation of Δ_b. The value of Δ_b in 7 T becomes finite at the charge ordering temperature (≈ 230 K), and rises with decrease in temperature. This increase in Δ_b saturates around T_N, which contrasts with the monotonous increase in the zero-field-cooled run [open circles in Fig. 10(a)]. These results imply that the charge ordering is weakened by the spin ordering in the $x=0.4$ crystal in 7 T. According to neutron-diffraction measurements for $Pr_{1-x}Ca_xMnO_3$ ($x=0.3$), with a similar spin-charge-orbital ordering by Yoshizawa *et al.*,[25] a superlattice peak intensity of (2,1.5,0) arising from the orbital ordering also saturates around T_N with a decrease at temperature in 2.5 T, while it shows a continuous increase in the zero field-cooled run. The present result is consistent with this neutron-diffraction observation, and clearly indicates that the order parameter of the CO state is suppressed by the antiferromagnetic spin ordering in a magnetic field. A recent high-magnetic-field study by Tokunaga *et al.*[35] reveals that the area of the CO state in the phase diagram expands below T_N in the $x=1/2$ sample (commensurate doping level). These experimental results lead to the conclusion that the commensurate *CE*-type spin ordering stabilizes the CO state, whereas the modified *CE* type, as shown in Fig. 1(b), weakens the robustness of the charge and orbital ordering. This also explains why the relatively low-field colossal MR effect is observed in the discommensurate $Pr_{1-x}Ca_xMnO_3$ system.

With a further decrease in temperature below T_N, Δ_b is gradually decreased and reaches zero at around 60 K. Such a continuous decrease of Δ_b with temperature is in contrast to the drastic change of ρ and M, but resembles the change in Δ_b and Δ_c seen in the field-increased and -decreased runs (see Fig. 7). The gradual variation of the gap feature is thus commonly observed prior to the complete collapse of the charge and orbital ordering.

IV. SUMMARY

We have observed a variation of optical spectra and their anisotropy with a change in temperature and magnetic field for a single crystal of $Pr_{1-x}Ca_xMnO_3(x=0.4)$. In the charge-ordered ground state (at 10 K), the respective optical conductivity spectra [$\sigma(\omega)$] for $\mathbf{E}\|b$ and $\mathbf{E}\|c$ have a different onset energy, Δ_b and Δ_c. The former reflects the electron hopping energy from Mn^{3+} to Mn^{4+} in the direction of $d_{3x^2-r^2}$ or $d_{3y^2-r^2}$ orbitals and the latter the transition energy of the extra electrons of $d_{3z^2-r^2}$ character along the c axis. The fact that Δ_c is smaller than Δ_b indicates that Δ_c can be viewed as the optical gap energy in the CO state (≈ 0.18 eV). Furthermore, an increase in number of optical-phonon modes is observed upon the charge ordering transition, as observed in $La_{1/2}Sr_{3/2}MnO_4$ with a similar CO state. As the temperature is increased from 10 K, Δ_b continuously decreases while Δ_c slightly increases up to T_N, and then decreases above T_N. This anomaly for Δ_c around T_N is due to the spin ordering structure of *modified CE* type, namely, antiferromagnetic in the ab plane but ferromagnetic along the c axis.

We have investigated the electronic-structural change accompanying the magnetic-field-induced insulator-metal transition at 30 K. Both the *b*- and *c*-polarized reflectivity spectra drastically change from an insulating low-reflectivity to a metallic high-reflectivity band at 7 T over a wide photon energy region (0.05–3 eV). The magnitude of Δ_b and Δ_c obtained from the respective $\sigma(\omega)$ gradually decreases with a magnetic field, and finally disappears at 6.5 T, indicating an almost continuous change in the electronic structure from the anisotropic CO state to the isotropic ferromagnetic metal in spite of the gigantic change of resistivity upon the complete melting transition of the CO state. In the field-decreased run from 7 T, both Δ values suddenly emerge around ≈ 4.5 T. Surprisingly, the clear anisotropic feature was not observed even once at zero field after the field-induced melting of the charge and orbital ordering, which probably results from the subsisting orbital disordering.

Such charge ordering and disordering transitions are also observed in the temperature-decreased run in magnetic fields, say 7 T. As the temperature decreases, the *b*-polarized $\sigma(\omega)$ becomes gaplike around 230 K due to the CO transition. The value of Δ_b increases with decrease in temperature from 230 K down to T_N, but rather decreases once the *modified CE*-type spin ordering [Fig. 1(b)] is realized. This result indicates that the spin ordering weakens the robustness of the CO state in an external magnetic field, which is consistent with the result of recent neutron-diffraction measurements.[25] With a further decrease in temperature, $\sigma(\omega)$ at 7 T is drastically transformed into a metallic spectrum around 60 K, in accord with the resistive transition to the ferromagnetic metallic state due to the reentrant charge disordering.

ACKNOWLEDGMENTS

We would like to thank N. Misu and K. Uchida for their technical assistance, and T. Katsufuji and H. Yoshizawa for enlightening discussions. The measurements of reflectivity spectra in vacuum ultraviolet region were performed at INS-SOR, Institute for Solid State Physics, the University of Tokyo. This work was supported in part by Grants-in-Aid for Scientific Research from the Ministry of Education, Science, Sport, and Culture, Japan, and by the New Energy and Industrial Technology Development Organization of Japan (NEDO).

[1] G. H. Jonker and J. H. van Santen, Physica (Amsterdam) **16**, 337 (1950).

[2] R. M. Kusters, D. A. Singleton, R. McGreevy, and W. Heyes, Physica B **155**, 362 (1989).

[3] K. Chahara, T. Ohno, M. Kasai, and Y. Kozono, Appl. Phys. Lett. **63**, 1990 (1993).

[4] R. von Helmolt, J. Wecker, B. Holzapfel, L. Schultz, and K. Samwer, Phys. Rev. Lett. **71**, 2331 (1993).

[5] M. McCormack, S. Jin, T. H. Tiefel, R. M. Fleming, J. M. Phillips, and R. Ramesh, Appl. Phys. Lett. **64**, 3045 (1994).
[6] S. Jin, T. H. Tiefel, M. McCormack, R. A. Fastnacht, R. Ramesh, and L. H. Chen, Science **264**, 413 (1994).
[7] H. L. Ju, C. Kwon, Qi Li, R. H. Greene, and T. Venkatesan, Appl. Phys. Lett. **65**, 2108 (1994).
[8] Y. Tokura, A. Urushibara, Y. Moritomo, A. Asamitsu, G. Kido, and N. Furukawa, J. Phys. Soc. Jpn. **63**, 418 (1994).
[9] A. Urushibara, Y. Moritomo, T. Arima, A. Asamitsu, G. Kido, and Y. Tokura, Phys. Rev. B **51**, 14 103 (1995).
[10] C. Zener, Phys. Rev. **82**, 403 (1951).
[11] P. W. Anderson and H. Hasegawa, Phys. Rev. **100**, 675 (1955).
[12] P.-G. de Gennes, Phys. Rev. **118**, 141 (1960).
[13] K. Kubo and N. Ohata, J. Phys. Soc. Jpn. **33**, 21 (1972).
[14] N. Furukawa, J. Phys. Soc. Jpn. **64**, 2734 (1995).
[15] A. J. Millis, P. B. Littlewood, and B. I. Shraiman, Phys. Rev. B **54**, 5405 (1996).
[16] H. Roder, J. Zang, and A. R. Bishop, Phys. Rev. Lett. **76**, 1356 (1996).
[17] Z. Jirak, S. Krupicka, Z. Simsa, M. Dlouha, and Z. Vlatislav, J. Magn. Magn. Mater. **53**, 153 (1985).
[18] Y. Tomioka, A. Asamitsu, H. Kuwahara, Y. Moritomo, and Y. Tokura, Phys. Rev. B **53**, R1689 (1996).
[19] Y. Tomioka, A. Asamitsu, Y. Moritomo, and Y. Tokura, J. Phys. Soc. Jpn. **64**, 3626 (1995).
[20] V. Kiryukhin, D. Casa, J. P. Hill, B. Keimer, A. Bigllante, Y. Tomioka, and Y. Tokura, Nature (London) **386**, 813 (1997).
[21] K. Miyano, T. Tanaka, Y. Tomioka, and Y. Tokura, Phys. Rev. Lett. **78**, 4257 (1997).
[22] Y. Okimoto, Y. Tokura, Y. Tomioka, Y. Onose, Y. Otsuka, and K. Miyano, Mol. Cryst. Liq. Cryst. **315**, 257 (1998).
[23] A. Asamistu, Y. Tomioka, and Y. Tokura, Nature (London) **388**, 50 (1997).
[24] J. P. Hill, Y. Murakami, Y. Tomioka, and Y. Tokura (unpublished).
[25] H. Yoshizawa, H. Kawano, Y. Tomioka, and Y. Tokura, Phys. Rev. B **52**, 13 145 (1995); J. Phys. Soc. Jpn. **52**, 3626 (1995).
[26] Y. Okimoto, Y. Tomioka, Y. Onose, Y. Otsuka, and Y. Tokura, Phys. Rev. B **57**, R9377 (1998).
[27] S. Yamaguchi, Y. Okimoto, K. Ishibashi, and Y. Tokura, Phys. Rev. B **58**, 6862 (1998).
[28] M. Couzi and P. V. Huang, J. Chim. Phys. Phys.-Chim. Biol. **69**, 1339 (1972).
[29] P. Calvani, A. Paolone, P. Dore, S. Lupi, P. Maselli, P. G. Medaglia, and S.-W. Cheong, Phys. Rev. B **54**, R9592 (1996); T. Ishikawa, K. Ohkura, and Y. Tokura (unpublished).
[30] T. Katsufuji, T. Tanabe, T. Ishikawa, Y. Fukuda, T. Arima, and Y. Tokura, Phys. Rev. B **54**, R14 230 (1996).
[31] S. G. Kaplan, M. Quijada, H. D. Drew, D. B. Tanner, G. C. Xiong, R. Ramesh, C. Kwon, and T. Venkatesan, Phys. Rev. Lett. **77**, 2081 (1996).
[32] S. Uchida, T. Ido, H. Takagi, T. Arima, Y. Tokura, and S. Tajima, Phys. Rev. B **43**, 7942 (1991).
[33] T. Katsufuji, Y. Okimoto, and Y. Tokura, Phys. Rev. Lett. **75**, 3497 (1995).
[34] Y. Okimoto, T. Katsufuji, T. Ishikawa, A. Urushibara, T. Arima, and Y. Tokura, Phys. Rev. Lett. **75**, 109 (1995).
[35] M. Tokunaga, N. Miura, Y. Tomioka, and Y. Tokura, Phys. Rev. B **57**, 5259 (1997).